

Classical Petermann Factor as a Measure of Quantum Squeezing in Photonic Time Crystals

Younsun Kim,^{1,*} Kyungmin Lee,^{1,*} Changhun Oh,¹ Young-Sik Ra,¹ Kun Woo Kim,^{2,†} and Bumki Min^{1,‡}

¹*Department of Physics, Korea Advanced Institute of Science and Technology, Daejeon 34141, Republic of Korea*

²*Department of Physics, Chung-Ang University, 06974 Seoul, Republic of Korea*

Photonic time crystals realize a continuum of momentum-resolved $SU(1,1)$ parametric amplifiers. We show that a classical quantity, the Petermann factor of the effective Floquet Bogoliubov-de Gennes (BdG) dynamical matrix, sets the scale of their quantum noise. In stable bands it fixes the Bogoliubov mixing and the vacuum quasiparticle population, while in momentum gaps it sets the photon-number prefactor and enhances the squeezing dynamics, with the Floquet growth rate setting the time scale. This converts classical measurements of mode nonorthogonality into quantitative predictions for squeezing and photon generation, and offers a compact design parameter for engineering quantum resources in two-mode BdG platforms.

Over the past several decades, two influential yet largely separate narratives have shaped our understanding of quantum noise in optical systems. One traces back to the observation that real lasers can exhibit noise and linewidths far exceeding the Schawlow–Townes prediction [1]. This discrepancy was explained in large part by recognizing that practical resonators are intrinsically non-Hermitian: their right and left eigenmodes are not orthogonal, and this non-orthogonality enhances the effective spontaneous emission and linewidth by a dimensionless amount now known as the Petermann factor (PF) [2–4]. Subsequent experiments on gain-guided and unstable cavities revealed that this factor can become remarkably large, particularly near exceptional points [5], and modern non-Hermitian photonics views it as a geometric measure of mode sensitivity [6, 7], linewidth broadening [8], and local density of states (LDOS) enhancement [9].

A parallel narrative emerged in quantum optics, where the development of two-photon coherent states, $SU(1,1)$ transformations, and optical parametric amplifiers established the concept of squeezed states [10–13]. In this framework, vacuum fluctuations are redistributed between conjugate quadratures, and the squeezing parameter quantifies the resulting noise reduction in the squeezed quadrature. It has evolved from a theoretical descriptor of minimum-uncertainty states into a practical resource for precision measurements, ranging from tabletop nonlinear optics experiments to gravitational-wave interferometry [14, 15].

Although both perspectives describe how fluctuations are reshaped and amplified, they have historically been expressed in different languages: the Petermann factor is usually formulated within classical non-Hermitian mode theory, whereas squeezing belongs to fully quantum, Hermitian dynamics, often formulated in an $SU(1,1)$ framework. Photonic time crystals (PTCs) [16–23] provide an ideal setting to unify these narratives. A PTC implements a continuum of momentum-resolved parametric amplifiers through periodic modulation of a homogeneous medium, producing momentum gaps (MGs) where Flo-

quet quasienergies become complex. Classical analyses reveal that the Petermann factor diverges as one approaches the MG edge, signaling non-Hermitian mode non-orthogonality, while recent quantum studies have associated the MG region with a dynamical Casimir-like effect [24, 25], leading to photon-pair creation and squeezing [26, 27]. As in other contexts, however, previous works on PTCs have treated the Petermann factor and squeezing separately: the Petermann factor has been used to explain non-Hermitian reshaping of the momentum-resolved photonic density of states (kDOS) near momentum-gap edges [28, 29], without connecting it to an explicit squeezing description.

In this Letter, we close this gap by developing a Bogoliubov-de Gennes (BdG) effective-Hamiltonian framework showing that the classical and quantum monodromy matrices are formally equivalent, and therefore share identical spectra and Petermann factors. As a result, the Petermann factor directly quantifies the degree of vacuum squeezing and quasiparticle population in the *band regime*, while inside the *momentum gap*, together with the Floquet growth rate—the imaginary part of the quasienergy—it acts as a prefactor that amplifies the initial rate of squeezing. Classical mode non-orthogonality thus manifests as enhanced quantum squeezing, and the Petermann factor extracted from the BdG dynamical matrix becomes a single control parameter for squeezing in a broad class of two-mode $SU(1,1)$ bosonic systems, with PTCs providing a particularly transparent and experimentally accessible realization.

We consider a one-dimensional PTC, a homogeneous medium whose permittivity $\varepsilon(t)$ is modulated periodically in time with period $T = 2\pi/\Omega$. The Hamiltonian of a quantum PTC in a specific pair of modes $(k, -k)$ can be expressed as [30]:

$$H_k(t) = A(t)(n_k + n_{-k} + 1) + B(t)(a_k a_{-k} + a_k^\dagger a_{-k}^\dagger), \quad (1)$$

where $n_k = a_k^\dagger a_k$ is the number operator for the k -mode. Here we adopt natural units, $\hbar = c = \varepsilon_0 = 1$. Also, $A(t) = k[1 + \varepsilon^{-1}(t)]/2$, $B(t) = k[1 - \varepsilon^{-1}(t)]/2$, where k

denotes the magnitude of the wavevector.

Then, it is natural to recast Eq. (1) into the BdG form, which leads to:

$$H_k(t) = \Phi^\dagger H_{\text{BdG}}(t) \Phi, \quad H_{\text{BdG}}(t) = \begin{bmatrix} A(t) & B(t) \\ B(t) & A(t) \end{bmatrix}, \quad (2)$$

where the Nambu basis is defined as $\Phi = (a_k, a_{-k}^\dagger)^\top$. The operator dynamics is governed by the Heisenberg equation of motion $\partial_t a_k = -i[a_k, H_k(t)]$, which in the Nambu basis yields $i\partial_t \Phi(t) = \mathcal{M}_q(t) \Phi(t)$. Here the dynamical matrix is given by $\mathcal{M}_q(t) \equiv \sigma_z H_{\text{BdG}}(t)$, with the Pauli- z matrix σ_z . Given the time periodicity $\mathcal{M}_q(t) = \mathcal{M}_q(t+T)$, the stroboscopic behavior of the operators is captured by the monodromy matrix $\mathcal{U}(T, 0) = \mathcal{T} \exp[-i \int_0^T \mathcal{M}_q(t) dt]$, where \mathcal{T} denotes the time-ordering operator. This allows us to define an effective BdG Hamiltonian $H_{\text{BdG}}^{\text{eff}}$ via the relation $\mathcal{U}(T, 0) = \exp[-i\sigma_z H_{\text{BdG}}^{\text{eff}} T]$.

Having established the quantum BdG framework, we now clarify its precise correspondence with the classical wave dynamics of the same time-modulated medium. A straightforward calculation shows that the quantum and classical monodromy matrices share the same eigenvalues [31]. Consequently, the Heisenberg evolution for the Nambu basis yields the same Floquet quasienergies as the corresponding classical wave dynamics. Since the quantum BdG evolution remains in the $SU(1, 1)$ group, its eigenvalues come in reciprocal pairs $\lambda_+ \lambda_- = 1$ and take the form $\lambda_\pm(k) = e^{\mp i\epsilon_k T}$ in the band (stable) regime and $\lambda_\pm(k) = -e^{\pm i\kappa_k T}$ in the MG (unstable) regime, where ϵ_k and κ_k are nonnegative real values representing the real quasienergy dispersion and the Floquet growth rate, respectively [31]. The resulting quasienergy spectrum, with ϵ_k and κ_k shown explicitly, is illustrated in Fig. D.1 [31]. Throughout, we refer to the band (stable) regime as the region $k < k_{c-}$ or $k > k_{c+}$, and to the MG (unstable) regime as $k_{c-} < k < k_{c+}$ [32].

The full effective Hamiltonian in the stable regime takes the form [31]

$$H_{\text{eff}} = \Phi^\dagger H_{\text{BdG}}^{\text{eff}} \Phi = \epsilon_k (b_k^\dagger b_k + b_{-k}^\dagger b_{-k} + 1), \quad (3)$$

where we set $S^{-1} \Phi \equiv (b_k, b_{-k}^\dagger)^\top$, with S being a Bogoliubov (symplectic) transformation that preserves the bosonic commutation relation $[b_k, b_{k'}^\dagger] = \delta_{kk'}$. With the parametrization $b_k = e^{i\theta} \cosh(r_k) a_k + \sinh(r_k) a_{-k}^\dagger$, the Bogoliubov transformation S diagonalizes $H_{\text{BdG}}^{\text{eff}}$, leading to Eq. (3). Thus the quasiparticle band ϵ_k appearing in the effective Hamiltonian is *exactly* the classical quasienergy band obtained from Maxwell's equations, establishing a direct classical-quantum correspondence at the level of the Floquet band structure [31].

Denoting $|R_k\rangle$ and $|L_k\rangle$ as the right and left eigenvectors of the effective dynamical matrix respectively, we define the Petermann factor (using the standard Euclidean

inner product in Nambu space) to be

$$K_k = \frac{\langle L_k | L_k \rangle \langle R_k | R_k \rangle}{|\langle L_k | R_k \rangle|^2}. \quad (4)$$

Due to the relation between the classical and quantum monodromy matrices [31], K_k simultaneously quantifies the non-orthogonality in both pictures. As shown in Fig. 1(a), K_k exhibits a sharp divergence as the momentum approaches the MG edges $k_{c\pm}$. While the classical interpretation links this divergence to non-Hermitian degeneracy, a crucial question remains: how does this classically defined non-Hermitian geometric factor manifest physically in the quantum regime? In what follows, we address this question separately in the band and gap regimes.

We now investigate the Petermann factor in detail by explicitly deriving it from the monodromy matrix. In the band regime $k < k_{c-}$ or $k > k_{c+}$, we have shown that the quasiparticle description allows the Hamiltonian to be written as Eq. (3). With this parameterization, the Petermann factor is given by [31]

$$K_k = \cosh^2 2r_k. \quad (5)$$

This relation dictates that the Petermann factor is solely governed by the Bogoliubov mixing parameter r_k (or equivalently, the squeezing parameter) that defines the quasiparticle mode b_k . Figure 1(b) shows the momentum dependence of r_k obtained from the stroboscopic time evolution; when viewed together with Fig. 1(a), this visually confirms this direct one-to-one correspondence in the band. As the momentum approaches the MG edge, r_k diverges rapidly, representing the extreme limit of the Bogoliubov mixing from the bare mode a_k .

The physical significance of this factor is elucidated in Ref. [28, 29], where the *effective* spontaneous emission (SE) decay rate $\Gamma_D(\omega)$ is shown to be proportional to $\sqrt{K_k}$ in the weak coupling regime. To interpret this in the quantum picture, we use the relation $\langle \hat{n}_{k,b} \rangle = \sinh^2 r_k$, where $\langle \hat{n}_{k,b} \rangle \equiv \langle 0 | b_k^\dagger b_k | 0 \rangle$ denotes the expectation value of the quasiparticle number in the photon vacuum state $|0\rangle$ (defined by $a_{\pm k} |0\rangle = 0$). This leads to

$$\langle \hat{n}_{k,b} \rangle = \frac{\sqrt{K_k} - 1}{2}. \quad (6)$$

Equivalently, $\sqrt{K_k} = 2 \langle \hat{n}_{k,b} \rangle + 1$, which provides an intuitive physical interpretation: in the band regime the Petermann factor quantifies the excess vacuum fluctuations through the mean *Bogoliubov quasiparticle* population in the photon vacuum. The additional unity term accounts for the vacuum baseline and restores the limit $\sqrt{K_k} = 1$ when $\langle \hat{n}_{k,b} \rangle = 0$. Fig. 1(b) illustrates this behavior of $\langle \hat{n}_{k,b} \rangle$, parametrized by the squeezing parameter r_k .

Having clarified the physical meaning of the Petermann factor in the band regime, we now turn to the

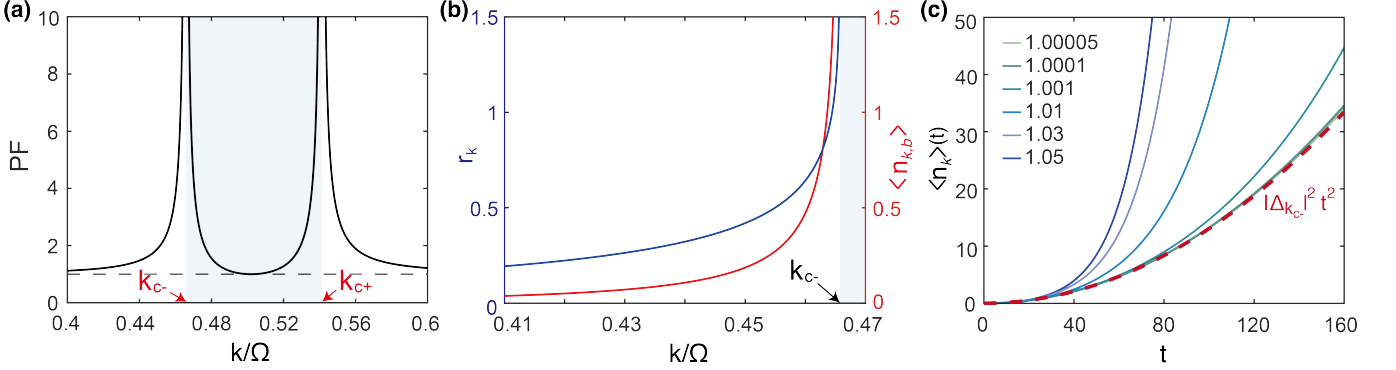


FIG. 1. (a) Petermann factor of a PTC with $\varepsilon^{-1}(t) = 1 - 2\alpha \cos \Omega t$, where $\alpha = 0.15$ and $\Omega = 1$. The blue shaded region indicates the MG (unstable) regime, and K_k diverges at the MG edges $k_{c\pm}$. The dashed line represents the lower bound $K_k = 1$. (b) Squeezing parameter r_k and the quasiparticle expectation value in the photon vacuum, $\langle \hat{n}_{k,b} \rangle$ in the band (stable) regime. As the momentum approaches the MG edge k_{c-} , both quantities increase with the Petermann factor K_k , as quantified by Eqs. (5) and (6). (c) Temporal evolution of the photon number $\langle \hat{n}_k(t) \rangle$ in the MG, obtained from the effective Floquet Hamiltonian. The curves represent stroboscopic evolution at integer multiples of T . Legends indicate the momentum ratio k/k_{c-} . As the system approaches the critical point ($k \rightarrow k_{c-}$), the dynamics follow the universal quadratic scaling $|\Delta_{k_{c-}}|^2 t^2$, illustrated by the red dashed line.

MG, where $k_{c-} < k < k_{c+}$ and mode amplification occurs. In this regime, the effective dynamical matrix $\mathcal{M}_q^{\text{eff}} = \sigma_z H_{\text{BdG}}^{\text{eff}}$ takes the form:

$$\mathcal{M}_q^{\text{eff}} = \begin{pmatrix} g_k & \Delta_k \\ -\Delta_k^* & -g_k \end{pmatrix} + \mathbb{I}\mu. \quad (7)$$

In general, $\mu = 0$ or π/T in the MG regime; in our case, we have $\mu = \pi/T$. The Floquet growth rate is then given by $\kappa_k = \sqrt{|\Delta_k|^2 - g_k^2}$, which requires the condition $|\Delta_k| > g_k$ [31].

With these parameters defined, the Petermann factor in the MG takes the form [31]

$$K_k = \frac{|\Delta_k|^2}{\kappa_k^2}. \quad (8)$$

This relation illustrates how the Petermann factor manifests itself in the squeezing dynamics. The stroboscopic evolution is captured by a time-dependent squeezing parameter $r_k(t)$, for which one finds the simple relation $\sinh r_k(t) = \sqrt{K_k} \sinh(\kappa_k t)$. It implies that, for a fixed parametric growth rate κ_k (which in PTCs corresponds to the Floquet growth rate), the Petermann factor enhances the initial squeezing rate by $\sqrt{K_k}$ [31]. We further show that intrinsic loss produces only subleading corrections in a short-time expansion; the Petermann-enhanced initial squeezing rate persists under symmetric Markovian damping [31]. Consequently, the average photon number generated from the initial vacuum state, $\langle \hat{n}_k(t) \rangle \equiv \langle 0 | \hat{a}_k^\dagger(t) \hat{a}_k(t) | 0 \rangle$, is given by

$$\langle \hat{n}_k(t) \rangle = K_k \sinh^2(\kappa_k t). \quad (9)$$

Hence, non-orthogonality appears as a multiplicative “gain factor” on vacuum amplification.

Even though the growth rate κ_k approaches 0 at the MG edge, the diverging Petermann factor compensates for the vanishing growth rate. As $\kappa_k \rightarrow 0$, the photon number exhibits a quadratic scaling, i.e. $\langle \hat{n}_k(t) \rangle \approx |\Delta_k|^2 t^2$. Since the characteristic time scale $\tau \sim \kappa_k^{-1}$ diverges at the MG edge, this quadratic behavior dominates the dynamics, as illustrated in Fig. 1(c).

We now delve deeper into the physical significance of the Petermann factor—intrinsically a non-Hermitian quantity—within the framework of Hermitian quantum mechanics. Beyond its role as a classical measure of mode non-orthogonality, our analysis shows that the Petermann factor acquires a meaning that goes beyond a simple comparison with a Hermitian reference. In the band regime, $K_k = 1$ corresponds to a Hermitian dynamical matrix that can be brought to $\sigma_z H_{\text{BdG}} = \text{diag}(g, -g)$; in this case the full Hamiltonian is $H = g(a_k^\dagger a_k + a_{-k}^\dagger a_{-k} + 1)$, which we take as the reference against which non-orthogonality is measured. In the momentum gap regime, by contrast, K_k approaches 1 when the dynamical matrix satisfies the anti-Hermitian relation $(\sigma_z H_{\text{BdG}})^\dagger = -(\sigma_z H_{\text{BdG}})$. Since H_{BdG} itself must remain Hermitian, its diagonal elements are real, which forbids purely imaginary diagonal entries in $\sigma_z H_{\text{BdG}}$; under this constraint, the corresponding reference Hamiltonian reduces to $H = (\Delta a_k a_{-k} + \text{h.c.})$. Deviations from these reference forms are precisely what K_k quantifies. Thus, in the $SU(1, 1)$ BdG formalism, it is not the full Hermitian Hamiltonian that inherits the non-Hermitian nature of the classical matrix. Instead, the non-Hermitian structure manifests at the level of the dynamical matrix governing the operator evolution [33]. Most importantly, the Petermann factor can be viewed as a measure of how far the dynamical matrix is from the Hermitian (band)

or anti-Hermitian (momentum gap) reference form, and hence as a quantifier of the degree of mixing between rotation and squeezing in the phase space [31, 34]. This result is not merely a parametrization: it identifies a map between a biorthogonal non-Hermitian metric (the Petermann factor) and the symplectic $SU(1, 1)$ squeezing parameter, with direct consequences for measurable quantum noise.

The central message of this work is that a classical nonorthogonality metric can be read as a quantitative quantum resource; PTCs provide a direct demonstration of this link. Because the classical field evolution and the quantum BdG dynamics are governed by formally equivalent Floquet monodromy matrices, K_k fixes the Bogoliubov mixing in stable bands, while in momentum gaps K_k and the Floquet growth rate κ_k jointly control the time-dependent photon generation. Since K_k (and κ_k in gaps) can be inferred from classical measurements, for example decay-rate enhancement or kDOS reshaping [28, 29], the corresponding squeezing and photon yield follow from the algebraic relations derived here. More broadly, this identifies biorthogonal mode geometry as a practical design knob for parametric quantum noise in a variety of quadratic bosonic platforms admitting an effective two-mode $SU(1, 1)$ BdG reduction [35–38]. In short, biorthogonality is not a nuisance here; it is the resource that sets the quantum noise and the resulting squeezing and photon yield.

We thank J. B. Pendry, P. A. Huidobro and T. F. Alldard for insightful discussions. This work is supported by the National Research Foundation of Korea (NRF) through the government of Korea (RS-2022-NR070636) and the Samsung Science and Technology Foundation (SSTF-BA240202). K.W.K. acknowledges financial support from the Basic Science Research Program through the NRF funded by the Ministry of Education (no. RS-2025-00521598) and the Korean Government (MSIT) (no. 2020R1A5A1016518). Y.-S.R. acknowledges the support from Institute of Information & Communications Technology Planning & Evaluation (IITP) grant (RS-2025-25464959). C.O. was supported by the NRF grants funded by the MSIT (No. RS-2024-00431768 and No. RS-2025-00515456) and the IITP grants funded by the MSIT (No. RS-2025-02283189, No. RS-2025-02263264, and No. RS-2025-25464990).

* These authors contributed equally to this work.

† kunx@cau.ac.kr

‡ bmin@kaist.ac.kr

[1] A. L. Schawlow and C. H. Townes, Infrared and optical masers, *Phys. Rev.* **112**, 1940 (1958).

[2] A. E. Siegman, Excess spontaneous emission in non-hermitian optical systems. i. laser amplifiers, *Phys. Rev. A* **39**, 1253 (1989).

[3] A. E. Siegman, Excess spontaneous emission in non-hermitian optical systems. ii. laser oscillators, *Phys. Rev. A* **39**, 1264 (1989).

[4] K. Petermann, Calculated spontaneous emission factor for double-heterostructure injection lasers with gain-induced waveguiding, *IEEE Journal of Quantum Electronics* **15**, 566 (1979).

[5] M. V. Berry, Mode degeneracies and the petermann excess-noise factor for unstable lasers, *Journal of Modern Optics* **50**, 63 (2003).

[6] J. Wiersig, Petermann factors and phase rigidities near exceptional points, *Phys. Rev. Res.* **5**, 033042 (2023).

[7] H. Schomerus, Eigenvalue sensitivity from eigenstate geometry near and beyond arbitrary-order exceptional points, *Phys. Rev. Res.* **6**, 013044 (2024).

[8] H. Wang, Y.-H. Lai, Z. Yuan, M.-G. Suh, and K. Vahala, Petermann-factor sensitivity limit near an exceptional point in a brillouin ring laser gyroscope, *Nature Communications* **11**, 1610 (2020).

[9] A. Pick, B. Zhen, O. D. Miller, C. W. Hsu, F. Hernandez, A. W. Rodriguez, M. Soljačić, and S. G. Johnson, General theory of spontaneous emission near exceptional points, *Opt. Express* **25**, 12325 (2017).

[10] H. P. Yuen, Two-photon coherent states of the radiation field, *Phys. Rev. A* **13**, 2226 (1976).

[11] K. Wodkiewicz and J. H. Eberly, Coherent states, squeezed fluctuations, and the $su(2)$ and $su(1,1)$ groups in quantum-optics applications, *J. Opt. Soc. Am. B* **2**, 458 (1985).

[12] C. M. Caves, Quantum-mechanical noise in an interferometer, *Phys. Rev. D* **23**, 1693 (1981).

[13] G. Gwak, C. Roh, Y.-D. Yoon, M. S. Kim, and Y.-S. Ra, Completely characterizing multimode second-order nonlinear optical quantum processes, *Nature Photonics* 10.1038/s41566-025-01787-x (2025), published online 11 Nov 2025; volume/pages may be assigned later.

[14] U. L. Andersen, T. Gehring, C. Marquardt, and G. Leuchs, 30 years of squeezed light generation, *Physica Scripta* **91**, 053001 (2016).

[15] J. Aasi *et al.*, Enhanced sensitivity of the ligo gravitational wave detector by using squeezed states of light, *Nature Photonics* **7**, 613 (2013).

[16] J. R. Zurita-Sánchez, P. Halevi, and J. C. Cervantes-González, Reflection and transmission of a wave incident on a slab with a time-periodic dielectric function (t), *Phys. Rev. A* **79**, 053821 (2009).

[17] N. Wang, Z.-Q. Zhang, and C. T. Chan, Photonic floquet media with a complex time-periodic permittivity, *Phys. Rev. B* **98**, 085142 (2018).

[18] E. Galiffi, R. Tirole, S. Yin, H. Li, S. Vezzoli, P. A. Huidobro, M. G. Silveirinha, R. Sapienza, A. Alù, and J. B. Pendry, Photonics of time-varying media, *Advanced Photonics* **4**, 10.1117/1.ap.4.1.014002 (2022).

[19] J. G. Gaxiola-Luna and P. Halevi, Temporal photonic (time) crystal with a square profile of both permittivity $\epsilon(t)$ and permeability $\mu(t)$, *Phys. Rev. B* **103**, 144306 (2021).

[20] M. A. Salem and C. Caloz, Temporal photonic crystals: Causality versus periodicity, in *2015 International Conference on Electromagnetics in Advanced Applications (ICEAA)* (2015) pp. 490–493.

[21] J. Park and B. Min, Spatiotemporal plane wave expansion method for arbitrary space-time periodic photonic media, *Opt. Lett.* **46**, 484 (2021).

[22] T. F. Allard, J. E. Sustaeta-Osuna, F. J. García-Vidal, and P. A. Huidobro, Broadband dipole absorption in dispersive photonic time crystals (2025), arXiv:2508.04619 [physics.optics].

[23] M. M. Asgari, P. Garg, X. Wang, M. S. Mirmoosa, C. Rockstuhl, and V. Asadchy, Theory and applications of photonic time crystals: a tutorial, *Adv. Opt. Photon.* **16**, 958 (2024).

[24] G. T. Moore, Quantum theory of the electromagnetic field in a variable-length one-dimensional cavity, *Journal of Mathematical Physics* **11**, 2679 (1970).

[25] V. Dodonov, Fifty years of the dynamical casimir effect, *Physics* **2**, 67 (2020).

[26] J. E. Sustaeta-Osuna, F. J. García-Vidal, and P. A. Huidobro, Quantum theory of photon pair creation in photonic time crystals, *ACS Photonics* **12**, 1873 (2025).

[27] J. Bae, K. Lee, B. Min, and K. W. Kim, Quantum electrodynamics of photonic time crystals, *Nature Communications* **17**, 858 (2026), published online 19 Dec 2025; version of record 22 Jan 2026.

[28] J. Park, K. Lee, R.-Y. Zhang, H.-C. Park, J.-W. Ryu, G. Y. Cho, M. Y. Lee, Z. Zhang, N. Park, W. Jeon, J. Shin, C. T. Chan, and B. Min, Spontaneous emission decay and excitation in photonic time crystals, *Phys. Rev. Lett.* **135**, 133801 (2025).

[29] K. Lee, M. Kyung, Y. Kim, J. Park, H. Lee, J. Choi, C. T. Chan, J. Shin, K. W. Kim, and B. Min, Spontaneous emission and lasing in photonic time crystals (2025), arXiv:2507.19916 [physics.optics].

[30] M. Lyubarov, Y. Lumer, A. Dikopoltsev, E. Lustig, Y. Sharabi, and M. Segev, Amplified emission and lasing in photonic time crystals, *Science* **377**, 425 (2022).

[31] See Supplemental Material for details in Secs. A–G, including the classical–quantum mapping of the monodromy matrix (A), $\mathfrak{su}(1, 1)$ algebra and stability classification (B–C), derivation of the stroboscopic effective Hamiltonian (D), Petermann-factor formulas and band/gap squeezing relations (E–F), and the lossy Heisenberg–Langevin extension (G).

[32] K. S. Eswaran, A. E. Kopaei, and K. Sacha, Aspects of quantum geometry in photonic time crystals (2025), arXiv:2511.17317 [physics.optics].

[33] R. Wakefield, A. Laing, and Y. N. Joglekar, Non-hermiticity in quantum nonlinear optics through symplectic transformations, *Applied Physics Letters* **124**, 201103 (2024).

[34] T. Figueiredo Roque, A. A. Clerk, and H. Ribeiro, Engineering fast high-fidelity quantum operations with constrained interactions, *npj Quantum Information* **7**, 28 (2021).

[35] J. R. Johansson, G. Johansson, C. M. Wilson, and F. Nori, Dynamical casimir effect in a superconducting coplanar waveguide, *Phys. Rev. Lett.* **103**, 147003 (2009).

[36] C. M. Wilson, G. Johansson, A. Pourkabirian, M. Simoen, J. R. Johansson, T. Duty, F. Nori, and P. Delsing, Observation of the dynamical casimir effect in a superconducting circuit, *Nature* **479**, 376 (2011).

[37] K. W. Murch, S. J. Weber, K. M. Beck, E. Ginossar, and I. Siddiqi, Reduction of the radiative decay of atomic coherence in squeezed vacuum, *Nature* **499**, 62 (2013).

[38] F. Hudelist, J. Kong, C. Liu, J. Jing, Z. Y. Ou, and W. Zhang, Quantum metrology with parametric amplifier-based photon correlation interferometers, *Nature Communications* **5**, 3049 (2014).

Supplemental Material: Classical Petermann Factor as a Measure of Quantum Squeezing in Photonic Time Crystals

Younsun Kim,^{1,*} Kyungmin Lee,^{1,*} Changhun Oh,¹ Young-Sik Ra,¹ Kun Woo Kim,^{2,†} and Bumki Min^{1,‡}

¹*Department of Physics, Korea Advanced Institute of Science and Technology, Daejeon 34141, Republic of Korea*

²*Department of Physics, Chung-Ang University, 06974 Seoul, Republic of Korea*

CONTENTS

A. Classical-to-quantum correspondence	1
B. $\mathfrak{su}(1,1)$ algebra and evolution	2
C. Stable vs unstable regime in $SU(1,1)$	2
D. Effective Hamiltonian and band correspondence	3
E. Petermann factor in quantum formalism	5
F. Petermann factor as a squeezing measure in the unstable regime	7
G. Effect of loss on the Petermann-squeezing relation	8
References	10

A. CLASSICAL-TO-QUANTUM CORRESPONDENCE

We consider a lossless electrodynamical system whose dynamics is governed by a Hamiltonian that is quadratic in the canonical fields (we set $\hbar = c = 1$). Starting from Maxwell's equations, which are first-order differential equations, one can introduce canonical variables such that the basis elements satisfy the Poisson bracket relation. In this canonical basis the dynamics takes the Nambu form

$$i \partial_t \begin{pmatrix} \alpha_k \\ \alpha_{-k}^* \end{pmatrix} = \mathcal{M} \begin{pmatrix} \alpha_k \\ \alpha_{-k}^* \end{pmatrix}, \quad (\text{S1})$$

with $\{\alpha_k, \alpha_{k'}^*\} = -i\delta_{kk'}$. Then, the direct quantization process $i\{\ , \ \} \rightarrow [\ , \]$ leads to the equation

$$i \partial_t \begin{pmatrix} \hat{a}_k \\ \hat{a}_{-k}^\dagger \end{pmatrix} = \mathcal{M} \begin{pmatrix} \hat{a}_k \\ \hat{a}_{-k}^\dagger \end{pmatrix}, \quad (\text{S2})$$

where $\mathcal{M} = \sigma_z H_{\text{BdG}}$, with H_{BdG} Hermitian. This indicates that the classical and quantum dynamics share the same dynamical matrix, and therefore share its spectrum $\{\omega_n\}$. This formalism can be naturally generalized to multimode systems, as the classical and quantum correspondence remains valid in general symplectic groups $Sp(2n, \mathbb{R})$ [1]. Moreover, \mathcal{M} is σ_z -pseudo-Hermitian, i.e.,

$$\mathcal{M}^\dagger \sigma_z = \sigma_z \mathcal{M}. \quad (\text{S3})$$

So its eigenvalues $\{\omega_n\}$ and corresponding eigenvectors $\{v_n\}$ satisfy

$$(\omega_m^* - \omega_n) v_m^\dagger \sigma_z v_n = 0. \quad (\text{S4})$$

That is, orthogonality is naturally defined with respect to the Krein inner product $\langle v_m, v_n \rangle_K := v_m^\dagger \sigma_z v_n$ rather than the Euclidean product $v_m^\dagger v_n$. In the case of a 2D matrix, for distinct real eigenvalues $\omega_1 \neq \omega_2 \in \mathbb{R}$, the eigenmodes

satisfy $\langle v_1, v_2 \rangle_K = 0$. If the eigenvalues form a non-real complex-conjugate pair, $\omega_2 = \omega_1^* \notin \mathbb{R}$, then $\langle v_1, v_1 \rangle_K = 0$ and $\langle v_2, v_2 \rangle_K = 0$.

However, in the case of a photonic time crystal (PTC), due to the time periodicity of its dynamical matrix, solving the eigenvalue problem of the instantaneous dynamical matrix does not give the desired physical modes of the system. Rather, we use the Floquet theorem and analyze the one-period evolution operator, namely the monodromy matrix $\mathcal{U}(T, 0)$, and solve its eigenvalue problem. As indicated in [2], we could use transfer matrix formalism to construct the monodromy matrix with the magnetic field amplitudes in direction $\pm k$.

Since $\mathbf{B}_k = i \mathbf{k} \times \mathbf{A}_k$, the same transfer matrix can be written for the vector potential amplitudes. Quantization is performed by promoting the canonical variables vector potential \mathbf{A} and $\mathbf{\Pi} = -\mathbf{D}$ to operators and imposing the equal-time canonical commutation relations. It enables the quantization of classical field basis into the bosonic annihilation and creation operator basis, forming a Nambu basis that inherits the identical transfer matrix structure.

B. $\mathfrak{su}(1, 1)$ ALGEBRA AND EVOLUTION

For any time interval, the evolution matrix is given as

$$\mathcal{U}(t_2, t_1) = \mathcal{T} \exp \left[-i \int_{t_1}^{t_2} \sigma_z H_{\text{BdG}}(t) dt \right]. \quad (\text{S5})$$

Here, the dynamical matrix is explicitly

$$\sigma_z H_{\text{BdG}}(t) = \begin{bmatrix} A(t) & B(t) \\ -B(t) & -A(t) \end{bmatrix}. \quad (\text{S6})$$

Meanwhile, the $\mathfrak{su}(1, 1)$ algebra can be defined with a basis

$$K_x = \frac{\sigma_x}{2}, \quad K_y = \frac{\sigma_y}{2}, \quad K_z = i \frac{\sigma_z}{2} \quad (\text{S7})$$

such that

$$[K_x, K_y] = K_z, \quad [K_y, K_z] = -K_x, \quad [K_z, K_x] = -K_y \quad (\text{S8})$$

The generator of the evolution can be written as $-i\sigma_z H_{\text{BdG}}(t) = 2[B(t)K_y - A(t)K_z]$ with real $A(t)$ and $B(t)$. Therefore, although the time-evolution operator involves a time-ordered exponential, the generator remains within the $\mathfrak{su}(1, 1)$ Lie algebra at all times, and the resulting evolution operator stays in the associated $SU(1, 1)$ group (up to an overall phase if an identity component is included).

C. STABLE VS UNSTABLE REGIME IN $SU(1, 1)$

If the evolution operator \mathcal{U} is an element of $SU(1, 1)$, we could parameterize it as follows:

$$\mathcal{U} = \begin{bmatrix} a & b \\ b^* & a^* \end{bmatrix}, \quad |a|^2 - |b|^2 = 1, \quad (\text{S9})$$

where a and b are complex numbers. Here, its characteristic polynomial is given as:

$$P(\lambda) = \lambda^2 - \text{Tr}(\mathcal{U})\lambda + 1. \quad (\text{S10})$$

Hence, letting two eigenvalues be λ_{\pm} , $\lambda_+ \lambda_- = 1$ holds. Imposing the trace condition, we could separate it into three cases:

$$\begin{cases} (\text{i}) |\text{Tr}(\mathcal{U})| < 2 & (\text{Elliptic}) \\ (\text{ii}) |\text{Tr}(\mathcal{U})| = 2 & (\text{Parabolic}) \\ (\text{iii}) |\text{Tr}(\mathcal{U})| > 2 & (\text{Hyperbolic}) \end{cases} \quad (\text{S11})$$

Solving the characteristic polynomial under the trace conditions in Eq. (S11), we obtain the following classifications of eigenvalues. In case (i), the eigenvalues form a complex-conjugate pair, and we could let $\lambda_{\pm} = e^{\pm i\theta}$, where $\theta \in \mathbb{R}$ defined modulo 2π . This corresponds to the stable regime. In case (ii), the eigenvalues are degenerate, $\lambda = \pm 1$; generically the matrix becomes non-diagonalizable, except for the trivial case $\mathcal{U} = \pm \mathbb{I}$. And in case (iii), the eigenvalue pair is purely real, and we could let it be λ and $1/\lambda$. It corresponds to the unstable regime.

D. EFFECTIVE HAMILTONIAN AND BAND CORRESPONDENCE

Here, we derive the explicit expression for the stroboscopic Hamiltonian for both stable and unstable regimes. In particular, by relating the Heisenberg dynamics in the Nambu basis to the effective Hamiltonian written in the Fock state basis, we show that the quasienergy spectrum emerges in a Bogoliubov spectrum-like form. First, briefly recall some basic facts about Floquet systems. The time periodicity of a dynamical matrix $\mathcal{M}(t) = \mathcal{M}(t + T)$ makes it possible to capture the stroboscopic behavior via the monodromy matrix $\mathcal{U}(T, 0) = \mathcal{T} \exp\left(-i \int_0^T \mathcal{M}(t) dt\right)$, where \mathcal{T} denotes the time-ordering operator. Here, the quasienergies $\{\nu_i\}$ are obtained from the eigenvalues of the monodromy matrix $\lambda_i = e^{-i\nu_i T}$ and are defined modulo $2\pi/T$.

We start from the observation that the monodromy matrix $\mathcal{U}_F \equiv \mathcal{U}(T, 0)$ belongs to the $SU(1, 1)$ group. In a stable regime, \mathcal{U}_F and $\text{diag}(e^{-iT\epsilon_k}, e^{iT\epsilon_k})$ are in the same conjugacy class [3]. That is, there exists $S \in SU(1, 1)$ such that

$$\mathcal{U}_F = S \begin{pmatrix} e^{-iT\epsilon_k} & 0 \\ 0 & e^{iT\epsilon_k} \end{pmatrix} S^{-1}. \quad (\text{S12})$$

We now take a matrix logarithm of \mathcal{U}_F and choose its branch such that the representative quasienergy lies in the Floquet Brillouin zone (FBZ) $(-\pi/T, \pi/T]$, which uniquely determines the quasienergy ϵ_k within this interval. The logarithm is then given by

$$\log \mathcal{U}_F = -iT \left[S \begin{pmatrix} \epsilon_k & 0 \\ 0 & -\epsilon_k \end{pmatrix} S^{-1} \right]. \quad (\text{S13})$$

Here, we define $\tilde{D} = \text{diag}(\epsilon_k, -\epsilon_k)$, which leads to the relation $S\tilde{D}S^{-1} = \sigma_z H_{\text{BdG}}^{\text{eff}}$ via $\mathcal{U}_F = e^{-iT\sigma_z H_{\text{BdG}}^{\text{eff}}}$. Now, we are ready to explicitly derive the form of H_{eff} . We can write the following relation:

$$\begin{aligned} H_{\text{eff}} &= \Phi^\dagger H_{\text{BdG}}^{\text{eff}} \Phi \\ &= \Psi^\dagger (S^\dagger H_{\text{BdG}}^{\text{eff}} S) \Psi \\ &= \Psi^\dagger (S^\dagger \sigma_z \cdot S \tilde{D} S^{-1} \cdot S) \Psi \\ &= \Psi^\dagger \underbrace{(S^\dagger \sigma_z S)}_{=\sigma_z \cdot :S \in SU(1,1)} \tilde{D} \Psi \\ &= \Psi^\dagger \sigma_z \tilde{D} \Psi \\ &= \Psi^\dagger \begin{pmatrix} \epsilon_k & 0 \\ 0 & \epsilon_k \end{pmatrix} \Psi \\ &= \epsilon_k (b_k^\dagger b_k + b_{-k}^\dagger b_{-k} + 1). \end{aligned} \quad (\text{S14})$$

Here we set $\Psi \equiv S^{-1} \Phi = (b_k, b_{-k}^\dagger)^\top$, where S is a symplectic transformation that preserves the bosonic commutation relation $[b_k, b_{k'}^\dagger] = \delta_{kk'}$. We have used the relation that the symplectic structure preserves the relation $S^\dagger \sigma_z S = \sigma_z$. Also, we should note that the Fock-state quasienergy spectrum shown in Fig. D.1(b) is calculated *before* FBZ folding. This representation naturally arises when we take the matrix logarithm of the monodromy operator to construct the effective Hamiltonian.

Now, we consider the unstable case, where the quasienergies become complex-valued. In this regime, the eigenvalues of \mathcal{U}_F are real and reciprocal, i.e., (λ, λ^{-1}) . Writing $\lambda = e^{-i\nu T}$, this implies that the quasienergies are given as $(\nu, -\nu)$ modulo $2\pi/T$. Since $\lambda, \lambda^{-1} \in \mathbb{R}$, the real part of ν (denoted by ϵ_k) must satisfy $e^{-i\epsilon_k T} = \pm 1$. Equivalently, denoting this value by $\mu \equiv \epsilon_k$ for brevity, $\mu = 0$ or π/T within the FBZ $(-\pi/T, \pi/T]$.

In Fig. D.1(a), the gray-shaded momentum gap region corresponds to $\mu = \pi/T$, yielding negative real eigenvalues. Consequently, the eigenvalue pair becomes $\lambda_\pm = -e^{\pm\kappa_k T}$. That is, $\text{Tr } \mathcal{U}_F = -2 \cosh(\kappa_k T) < -2$. Here as well, we note that the monodromy matrix $\mathcal{U}_F \in SU(1, 1)$ having eigenvalue pair $\lambda_\pm = e^{\pm\kappa_k T - i\mu T}$ is conjugate to the following canonical hyperbolic representative within the group [3]:

$$e^{-i\mu T \mathbb{I}} \begin{pmatrix} \cosh \kappa_k T & \sinh \kappa_k T \\ \sinh \kappa_k T & \cosh \kappa_k T \end{pmatrix} = e^{\kappa_k T \sigma_x - i\mu T \mathbb{I}}. \quad (\text{S15})$$

Moreover, the hyperbolic elements are not conjugate to any diagonal matrix in $SU(1, 1)$, since diagonal matrices in $SU(1, 1)$ must have unit-modulus eigenvalues $e^{\pm i\theta}$, by the group definition. Consequently, in the unstable regime,

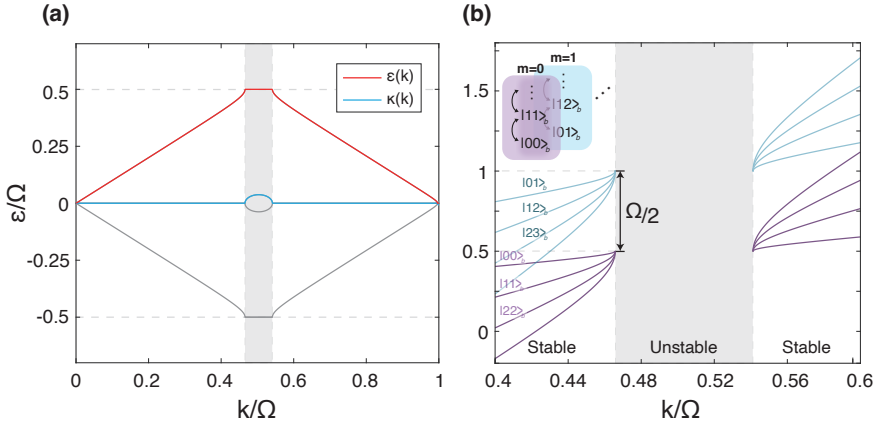


FIG. D.1. (a) Floquet band structure inside Floquet Brillouin zone (FBZ) from quantum BdG dynamical matrix. The gray-shaded region indicates the momentum gap (MG), and ϵ_k and κ_k indicate the real and imaginary part of the quasienergy, respectively. (b) Spectrum obtained from the effective Hamiltonian H_{eff} . The gray-shaded region indicates the MG, while blue and purple lines denote the spectrum for the momentum sectors $q = 1$ and $q = 0$, respectively. The discrete branches correspond to the Fock-state energy levels $(n_k + m_{-k} + 1)\epsilon_k$.

\mathcal{U}_F cannot be diagonalized by any symplectic similarity transformation $S \in SU(1,1)$ which preserves the bosonic commutation relation.

Diagonalization in this regime requires a non-symplectic similarity transformation and therefore does not preserve the bosonic commutation relations. Although such a transformation is unphysical in the sense discussed above, we introduce the following relation for convenience:

$$e^{\kappa_k T \sigma_x} = V \text{diag}(e^{\kappa_k T}, e^{-\kappa_k T}) V^{-1}, \quad (\text{S16})$$

where $V = \frac{1}{\sqrt{2}} \begin{pmatrix} 1 & 1 \\ 1 & -1 \end{pmatrix} \notin SU(1,1)$. Together with Eq. (S15), we know that there exists $S \in SU(1,1)$ such that

$$\begin{aligned} \mathcal{U}_F &= S \exp[\kappa_k T \sigma_x - iT \mu \mathbb{I}] S^{-1} \\ &= (SV) \begin{pmatrix} e^{T\kappa_k - iT\mu} & 0 \\ 0 & e^{-T\kappa_k - iT\mu} \end{pmatrix} (SV)^{-1} \end{aligned} \quad (\text{S17})$$

Taking the logarithm yields the following result.

$$\log \mathcal{U}_F = -iT[S(i\kappa_k \sigma_x + \mu \mathbb{I})S^{-1}]. \quad (\text{S18})$$

Here we have used the relation $V\sigma_z V^{-1} = \sigma_x$. By a similar argument discussed in the previous case, we can let $\Psi \equiv S^{-1}\Phi = (b_k, b_{-k}^\dagger)^\top$, and derive the effective Hamiltonian H_{eff} . It turns out that the result is as follows:

$$H_{\text{eff}} = i\kappa_k(b_k^\dagger b_{-k}^\dagger - b_{-k} b_k) + \mu(b_k^\dagger b_k - b_{-k}^\dagger b_{-k}) - \mu. \quad (\text{S19})$$

Consequently, this is the regime where the system cannot be diagonalized into a stable harmonic oscillator form. Instead, Eq. (S15) identifies the canonical hyperbolic representative of \mathcal{U}_F , and Eq. (S18) yields the corresponding effective dynamical matrix $i\kappa_k \sigma_x + \mu \mathbb{I}$ in the transformed basis $\Psi = S^{-1}\Phi$. Up to the identity shift $\mu \mathbb{I}$, the nontrivial part $i\kappa_k \sigma_x$ serves as the reference dynamical matrix in the unstable regime, as introduced in Sec. F.

At this point, it is worth emphasizing that ϵ_k and κ_k are the quasienergy spectrum that we have obtained from the classical spectrum. This equivalence is a direct consequence of the classical-to-quantum correspondence established in Sec. A, which ensures that both the classical and the quantum BdG operator dynamics are governed by the same dynamical matrix. Fig. D.1(a) shows this shared spectrum, which is obtained from the monodromy matrix. Since it remains in the $SU(1,1)$ group, the eigenvalue pair of the monodromy matrix is given as

$$\lambda_+ \lambda_- = 1, \quad \lambda_{\pm}(k) = \begin{cases} e^{\mp i\epsilon_k T} & (k \notin \text{MG}) \\ e^{\pm \kappa_k T - iT\mu} & (k \in \text{MG}) \end{cases}, \quad (\text{S20})$$

where MG denotes the momentum-gap region. In our system, the MG region corresponds to the unstable regime, whereas the band region ($k \notin \text{MG}$) corresponds to the stable regime. Interpreting the effective Hamiltonian H_{eff} , inside the band the system clearly has $\{|n_k, m_{-k}\rangle_b\}_{n,m}$ as its Floquet eigenstate at each mode, and has its corresponding quasienergy $(n_k + m_{-k} + 1)\epsilon_k$. Because the original Hamiltonian is given as $H_k(t) = \bigoplus_q H_q(t)$, where integer q indicates the number-difference sector, i.e., $q = n_k - n_{-k}$, we can treat each sector separately. As shown in Fig. D.1(b), the spectrum collapses within each sector q at the MG edge. This collapsing nature is inherited from the BdG spectrum, in which at the momentum gap edge, $\epsilon_k \rightarrow \Omega/2$.

E. PETERMANN FACTOR IN QUANTUM FORMALISM

In this section, we investigate the role of the Petermann factor (PF) in the quantum regime. The PF was originally introduced in the context of classical non-Hermitian systems as a measure of mode non-orthogonality, and can be consistently defined for the classical monodromy matrix in Floquet systems. The PF K_k defined for each mode has the form

$$K_k = \frac{\langle L_k | L_k \rangle \langle R_k | R_k \rangle}{|\langle L_k | R_k \rangle|^2}, \quad (\text{S21})$$

where the right eigenvector $|R_k\rangle$ is defined via

$$\mathcal{U}_F |R_k\rangle = \lambda_k |R_k\rangle, \quad (\text{S22})$$

and its corresponding left eigenvector $\langle L_k|$ is defined as

$$\langle L_k | \mathcal{U}_F = \langle L_k | \lambda_k. \quad (\text{S23})$$

This mode overlap is a classical quantity, but due to the correspondence discussed in Sec A, it directly relates to the quantities in the quantum BdG matrix as well. We separate it into two cases: stable and unstable case to see how the PF manifests itself in each regime.

First, we consider the case in the stable regime, where the monodromy matrix can be diagonalized by a similarity transformation

$$\mathcal{U}_F = S \begin{pmatrix} e^{-iT\epsilon_k} & 0 \\ 0 & e^{iT\epsilon_k} \end{pmatrix} S^{-1}, \quad (\text{S24})$$

with $S \in SU(1, 1)$. Then, we can parameterize S as

$$S = \begin{pmatrix} e^{-i\alpha} \cosh r_k & -e^{i\beta} \sinh r_k \\ -e^{-i\beta} \sinh r_k & e^{i\alpha} \cosh r_k \end{pmatrix}, \quad S^{-1} = \begin{pmatrix} e^{i\alpha} \cosh r_k & e^{i\beta} \sinh r_k \\ e^{-i\beta} \sinh r_k & e^{-i\alpha} \cosh r_k \end{pmatrix}, \quad (\text{S25})$$

and it naturally implies that the Bogoliubov operator takes the form

$$b_k = e^{i\alpha} \cosh r_k a_k + e^{i\beta} \sinh r_k a_{-k}^\dagger \quad (\text{S26})$$

$$b_{-k}^\dagger = e^{-i\beta} \sinh r_k a_k + e^{-i\alpha} \cosh r_k a_{-k}^\dagger. \quad (\text{S27})$$

Here, the relation $SD = \mathcal{U}_F S$ directly gives the relation of the right eigenvector v_i , i.e.,

$$\lambda_i v_i = \mathcal{U}_F v_i, \quad S = [v_1, v_2], \quad (\text{S28})$$

and the relation $DS^{-1} = S^{-1}\mathcal{U}_F$ gives the left eigenvector w_i^\dagger defined by

$$w_i^\dagger \lambda_i = w_i^\dagger \mathcal{U}_F, \quad S^{-1} = \begin{bmatrix} w_1^\dagger \\ w_2^\dagger \end{bmatrix}. \quad (\text{S29})$$

A straightforward calculation yields

$$\langle R^\pm | R^\pm \rangle = \cosh^2 r_k + \sinh^2 r_k = \cosh 2r_k \quad (\text{S30})$$

$$\langle L^\pm | L^\pm \rangle = \cosh 2r_k \quad (\text{S31})$$

$$\langle L^\pm | R^\pm \rangle = \cosh^2 r_k - \sinh^2 r_k = 1, \quad (\text{S32})$$

which gives the relation $K_k = \cosh^2 2r_k$.

Meanwhile, the result can be recast in a different form as well. Within the same parameterization as in Eq. (S25), the effective dynamical matrix $\mathcal{M}_q^{\text{eff}} \equiv \sigma_z H_{\text{BdG}}^{\text{eff}}$ defined via

$$\begin{aligned}\mathcal{U}(T, 0) &= \mathcal{T} \exp \left[-i \int_0^T \mathcal{M}_q(t) dt \right] \\ &= \exp \left[-i \sigma_z H_{\text{BdG}}^{\text{eff}} T \right]\end{aligned}\quad (\text{S33})$$

can be explicitly written as

$$\begin{aligned}\mathcal{M}_q^{\text{eff}} &= \epsilon_k \begin{pmatrix} \cosh 2r_k & e^{-i(\alpha-\beta)} \sinh 2r_k \\ -e^{i(\alpha-\beta)} \sinh 2r_k & -\cosh 2r_k \end{pmatrix} \\ &\equiv \begin{pmatrix} g_k & \Delta_k \\ -\Delta_k^* & -g_k \end{pmatrix},\end{aligned}\quad (\text{S34})$$

and therefore

$$H_{\text{BdG}}^{\text{eff}} = \begin{pmatrix} g_k & \Delta_k \\ \Delta_k^* & g_k \end{pmatrix}. \quad (\text{S35})$$

Here, we parameterize the matrix elements by g_k and Δ_k , where the condition $g_k > |\Delta_k|$ follows directly from $\cosh 2r_k > \sinh 2r_k$ and satisfies the relation $\epsilon_k = \sqrt{g_k^2 - |\Delta_k|^2}$. The PF can therefore be recast as:

$$K_k = \frac{g_k^2}{g_k^2 - |\Delta_k|^2} = \frac{g_k^2}{\epsilon_k^2}. \quad (\text{S36})$$

Now, consider the case of an unstable regime. As mentioned in Sec. D, the monodromy matrix in an unstable regime can be diagonalized as

$$\mathcal{U}_F = -(SV) \text{diag}(e^{T\kappa_k}, e^{-T\kappa_k})(SV)^{-1}, \quad (\text{S37})$$

and the effective dynamical matrix is parametrized into

$$\mathcal{M}_q^{\text{eff}} = S(i\kappa_k \sigma_x + \mu \mathbb{I}) S^{-1} \quad (\text{S38})$$

$$\equiv \begin{pmatrix} g_k & \Delta_k \\ -\Delta_k^* & -g_k \end{pmatrix} + \mu \mathbb{I}, \quad (\text{S39})$$

with parameters g_k and Δ_k , satisfying $g_k < |\Delta_k|$. Since $S \in SU(1, 1)$, parametrization analogous to Eq. (S25) can be applied to Eq. (S38), which gives

$$\begin{aligned}g_k &= \kappa_k \sin(\alpha + \beta) \sinh 2\eta_k \\ \Delta_k &= i\kappa_k e^{-2i\alpha} (\cosh^2 \eta_k - e^{2i(\alpha+\beta)} \sinh^2 \eta_k).\end{aligned}\quad (\text{S40})$$

It directly leads to the relation $|\Delta_k|^2 - g_k^2 = \kappa_k^2$, where κ_k denotes the imaginary part of the quasienergy spectrum.

Now, we derive an explicit form of the PF in an unstable regime. We start with the fact that the right eigenvectors $|R_k^\pm\rangle$ satisfy the relation

$$\mathcal{U}_F |R_k^\pm\rangle = -e^{\pm T\kappa_k} |R_k^\pm\rangle. \quad (\text{S41})$$

Based on this relation, we establish the relationship between the left and right eigenvectors. Omitting the mode index for brevity, the derivation proceeds as:

$$\begin{aligned}(\langle R^\pm | \sigma_z) \mathcal{U}_F &= \langle R^\pm | (\mathcal{U}_F^\dagger)^{-1} \sigma_z \\ &= (\mathcal{U}_F^{-1} |R^\pm\rangle)^\dagger \sigma_z \\ &= -e^{\mp T\kappa_k} \langle R^\pm | \sigma_z\end{aligned}\quad (\text{S42})$$

where the first line follows from the σ_z -pseudo-unitarity $\mathcal{U}_F^\dagger \sigma_z \mathcal{U}_F = \sigma_z$. In the final step, we used the fact that $|R^\pm\rangle$ having their eigenvalue $\lambda_\pm = -e^{\pm T\kappa_k}$ is an eigenvector of \mathcal{U}_F^{-1} with the reciprocal eigenvalue $\lambda_\pm^{-1} = -e^{\mp T\kappa_k}$. This confirms the relation that we can set the left eigenvector as $\langle L^\pm | = \langle R^\mp | \sigma_z$ in an unstable regime.

Then we can reformulate the form of the PF in an unstable regime as follows:

$$K_k = \frac{\langle R^\mp | R^\mp \rangle \langle R^\pm | R^\pm \rangle}{|\langle R^\mp | \sigma_z | R^\pm \rangle|^2}. \quad (\text{S43})$$

Rather than solving the eigenvalue problem with the monodromy matrix, we can work with the effective dynamical matrix, omitting the identity term $\mu\mathbb{I}$. That is,

$$\begin{pmatrix} g_k & \Delta_k \\ -\Delta_k^* & -g_k \end{pmatrix} |R_k^\pm\rangle = \pm i\kappa_k |R_k^\pm\rangle. \quad (\text{S44})$$

Then, the right eigenvectors can be written as

$$|R_k^+\rangle = \sqrt{N} \begin{pmatrix} \Delta_k \\ i\kappa_k - g_k \end{pmatrix}, \quad |R_k^-\rangle = \sqrt{M} \begin{pmatrix} -\Delta_k \\ i\kappa_k + g_k \end{pmatrix}, \quad (\text{S45})$$

with normalization constants \sqrt{N} and \sqrt{M} . Then, straightforward calculation yields

$$\begin{aligned} \langle R^+ | R^+ \rangle &= N\{|\Delta_k|^2 + (g_k^2 + \kappa_k^2)\} \\ &= 2N|\Delta_k|^2 \end{aligned} \quad (\text{S46})$$

$$\langle R^- | R^- \rangle = 2M|\Delta_k|^2 \quad (\text{S47})$$

$$\begin{aligned} \langle L^\pm | R^\pm \rangle &= \langle R^\pm | \sigma_z | R^\mp \rangle \\ &= \sqrt{NM}\{(-|\Delta_k|^2 + g_k^2 - \kappa_k^2) \pm i(2g_k\kappa_k)\} \\ &= 2\sqrt{NM}\{-\kappa_k^2 \pm ig_k\kappa_k\}. \end{aligned} \quad (\text{S48})$$

Eq. (S48) gives $|\langle R^\pm | \sigma_z | R^\mp \rangle|^2 = 4NM\kappa_k^2|\Delta_k|^2$, and therefore, satisfies the relation

$$K_k = \frac{|\Delta_k|^2}{\kappa_k^2}. \quad (\text{S49})$$

Consequently, we can express the Petermann factor in a unified form depending on the ratio between g_k and $|\Delta_k|$:

$$K_k = \begin{cases} \frac{1}{1 - |\Delta_k|^2/g_k^2} & (k \notin \text{MG}) \\ \frac{1}{1 - g_k^2/|\Delta_k|^2} & (k \in \text{MG}), \end{cases} \quad (\text{S50})$$

with $g_k^2/|\Delta_k|^2$ being a dimensionless parameter, where $|\Delta_k|^2 < g_k^2$ inside the band (stable) and $|\Delta_k|^2 > g_k^2$ in the momentum gap (unstable). Importantly, Eq. (S50) is not specific to PTCs: it holds for any *static* two-mode quadratic bosonic Hamiltonian whose BdG dynamical matrix can be written as $\sigma_z H_{\text{BdG}} = \begin{pmatrix} g & \Delta \\ -\Delta^* & -g \end{pmatrix}$. In PTCs, the parameters g_k and Δ_k are defined as the matrix elements of the *effective* dynamical matrix $\sigma_z H_{\text{BdG}}^{\text{eff}}$. Hence, the same logic leads to Eq. (S50) both for stable ($|\Delta| < g$) and unstable ($|\Delta| > g$) regimes.

F. PETERMANN FACTOR AS A SQUEEZING MEASURE IN THE UNSTABLE REGIME

In this section, we investigate how the Petermann factor manifests itself in the squeezing parameter in an unstable regime. Here, for the general discussion, we consider the static Hamiltonian given by

$$H_0 = g(n_k + n_{-k} + 1) + (\Delta^* a_k a_{-k} + \text{h.c.}). \quad (\text{S51})$$

Then the dynamical matrix that governs the Nambu operator dynamics, i.e., $i\partial_t \Phi = \sigma_z H_{\text{BdG}} \Phi$, $\Phi = (a_k, a_{-k}^\dagger)^\top$ is given as follows:

$$\sigma_z H_{\text{BdG}} = \begin{pmatrix} g & \Delta \\ -\Delta^* & -g \end{pmatrix}. \quad (\text{S52})$$

First, we define the growth rate $\kappa = \sqrt{|\Delta|^2 - g^2}$ in the unstable regime $|\Delta| > g$. Following Sec. E, the Petermann factor reads

$$K = \frac{|\Delta|^2}{\kappa^2} = \frac{1}{1 - g^2/|\Delta|^2}. \quad (\text{S53})$$

Meanwhile, the evolution $\mathcal{U}(t, 0)$ takes the form

$$\begin{aligned} \mathcal{U}(t, 0) &= \exp\{(-it\sigma_z H_{\text{BdG}})\} \\ &= \cosh(\kappa t)\mathbb{I} - i\frac{\sinh(\kappa t)}{\kappa}(\sigma_z H_{\text{BdG}}). \end{aligned} \quad (\text{S54})$$

From here, we obtain the relation of the two-mode squeezing parameter $r(t) = \text{arcsinh}(\frac{|\Delta|}{\kappa} \sinh(\kappa t))$, i.e.,

$$r(t) = \text{arcsinh}(\sqrt{K} \sinh(\kappa t)). \quad (\text{S55})$$

To gain physical insight, we first consider the regime where $K \approx 1$, i.e., $|\Delta|^2 \gg g^2$. Eq. (S51) and (S52) directly gives that such a case is where $H_0 \approx \Delta^* a_k a_{-k} + \text{h.c.}$. In this limit, the two-mode squeezing parameter grows linearly in time, i.e., $r(t) \approx \kappa t$.

Next, we consider the general case where $K > 1$. In this regime, the previous approximation no longer holds, and the squeezing parameter obeys the relation given in Eq. (S55).

In the short-time limit $\kappa t \ll 1$, using the approximation $\sinh \kappa t \approx \kappa t$, the squeezing parameter approximates into $r(t) \approx \sqrt{K} \kappa t$. Consequently, the initial growth rate is given as

$$\frac{dr}{dt} \Big|_{t \rightarrow 0} \approx \sqrt{K} \kappa. \quad (\text{S56})$$

Thus, for a fixed growth rate κ , the Petermann factor K enhances the initial squeezing process, resulting in a growth rate that is \sqrt{K} times larger than that of the case $K = 1$.

Now, based on the above discussions, we further clarify the meaning of the PF in the unstable regime. For this, we introduce a reference dynamical matrix

$$\mathcal{M}_{\text{ref}} = \begin{pmatrix} 0 & i\kappa \\ i\kappa & 0 \end{pmatrix}, \quad (\text{S57})$$

which represents a system with the growth rate κ , and Petermann Factor $K = 1$. Up to a trivial identity shift $\mu\mathbb{I}$, any dynamical matrix in the unstable class with the same growth rate κ can be related to this reference form $\mathcal{M}_{\text{ref}} = i\kappa\sigma_x$ via a similarity transformation $\sigma_z H_{\text{BdG}} = S\mathcal{M}_{\text{ref}} S^{-1}$ where $S \in SU(1, 1)$ [3]. Within this framework, the PF can be interpreted as a prefactor that quantifies the deviation from the reference matrix \mathcal{M}_{ref} . While the growth rate κ remains invariant under a transformation S , the degree of basis change induced by S determines the magnitude of K , causing the initial growth rate to be amplified by a factor \sqrt{K} .

In the case of an unstable regime of PTCs, the effective dynamical matrix is given by Eq. (S18). Consequently, in the Bogoliubov basis $\Psi = S^{-1}\Phi \equiv (b_k, b_{-k}^\dagger)^\top$ introduced in Sec. D, the dynamical matrix is transformed into the reference form $i\kappa\sigma_x + \mu\mathbb{I}$ up to the identity shift $\mu\mathbb{I}$. Hence, the b -operator basis in Sec. D can be viewed as a canonical *reference squeezing basis* in which the transformed effective dynamical matrix takes the standard form \mathcal{M}_{ref} .

G. EFFECT OF LOSS ON THE PETERMANN-SQUEEZING RELATION

We now investigate the robustness of the Petermann-enhanced initial squeezing rate against intrinsic loss. Here we consider the Heisenberg-Langevin equations, which are given by

$$\begin{aligned} \partial_t a_1 &= \left[-ig - \frac{\gamma}{2} \right] a_1 - i\Delta a_2^\dagger + \sqrt{\gamma} a_{1,\text{in}} \\ \partial_t a_2^\dagger &= \left[ig - \frac{\gamma}{2} \right] a_2^\dagger + i\Delta^* a_1 + \sqrt{\gamma} a_{2,\text{in}}^\dagger, \end{aligned} \quad (\text{S58})$$

assuming linear loss $\gamma_1 = \gamma_2 \equiv \gamma$ and coupling to a Markovian vacuum bath. Then the corresponding noise operators satisfy the relations

$$\begin{aligned}\langle a_{\mu,\text{in}}(t) a_{\nu,\text{in}}^\dagger(t') \rangle &= \delta_{\mu\nu} \delta(t - t'), \\ \langle a_{\mu,\text{in}}^\dagger(t) a_{\nu,\text{in}}(t') \rangle &= 0, \\ \langle a_{\mu,\text{in}}(t) a_{\nu,\text{in}}(t') \rangle &= 0.\end{aligned}\tag{S59}$$

Casting the equations in the matrix form gives

$$\frac{d}{dt} \begin{pmatrix} a_1 \\ a_2^\dagger \end{pmatrix} = -i \left[\mathcal{M} - i \frac{\gamma}{2} \mathbb{I} \right] \begin{pmatrix} a_1 \\ a_2^\dagger \end{pmatrix} + \sqrt{\gamma} \begin{pmatrix} a_{1,\text{in}} \\ a_{2,\text{in}}^\dagger \end{pmatrix}.\tag{S60}$$

Solving the eigenvalue problem $\det(\mathcal{M} - (\lambda + i \frac{\gamma}{2}) \mathbb{I}) = 0$ yields $\lambda_{\pm} = \pm \sqrt{g^2 - |\Delta|^2} - i\gamma/2$, and the threshold limit, marking the transition to the newly defined unstable regime (where $\exists \lambda$ s.t. $\Im(\lambda) > 0$) is determined by

$$|\Delta|^2 - g^2 = \gamma^2/4.\tag{S61}$$

Now, it is natural to classify the parameter space into three distinct regimes: (i) $g > |\Delta|$, corresponding to the elliptic regime discussed in Eq. (S11), (ii) $g^2 < |\Delta|^2 < g^2 + \gamma^2/4$, representing the hyperbolic regime below the threshold, and (iii) $|\Delta|^2 > g^2 + \gamma^2/4$, which corresponds to the regime above the threshold. Note that the exceptional point remains unchanged, but the stationary solution exists in the regimes (i) and (ii).

Meanwhile, for symmetric linear loss, the matrix is shifted by $-\mathbb{I}\gamma/2$. Therefore the Petermann factor determined by the eigenvector biorthogonality remains unchanged, while the imaginary parts of the eigenvalues shift by $-\gamma/2$.

Assuming an initial vacuum state, we solve the dynamics of $\langle a_1^\dagger a_1 \rangle = \langle a_2^\dagger a_2 \rangle \equiv n$ and $\langle a_1 a_2 \rangle \equiv m$, governed by the coupled equations

$$\begin{aligned}\frac{dn}{dt} &= -\gamma n + i\Delta^* m - i\Delta m^* \\ \frac{dm}{dt} &= -(2ig + \gamma)m - i\Delta(2n + 1).\end{aligned}\tag{S62}$$

Then the general solution is given by

$$\begin{aligned}n(t) &= \frac{2|\Delta|^2}{\gamma^2 - 4(|\Delta|^2 - g^2)} \left[1 - e^{-\gamma t} \left(\cosh(2\kappa t) + \frac{\gamma}{2\kappa} \sinh(2\kappa t) \right) \right] \\ |m(t)| &= \frac{1}{|\Delta|} \sqrt{(gn)^2 + \frac{1}{4}(\gamma n + \dot{n})^2},\end{aligned}\tag{S63}$$

where $\sqrt{|\Delta|^2 - g^2} \equiv \kappa$. Note that it is the general solution for all cases (i) – (iii). In the regime where $|\Delta|^2 < g^2$, substituting $\kappa = i\epsilon$ transforms the hyperbolic functions into trigonometric functions via the identities $\cosh(2i\epsilon t) = \cos(2\epsilon t)$ and $\sinh(2i\epsilon t) = i \sin(2\epsilon t)$.

Expanding $n(t)$ to the third order yields

$$n(t) = |\Delta|^2(t^2 - \frac{2\gamma}{3}t^3) + \mathcal{O}(t^4),\tag{S64}$$

which shows that the loss γ enters as a third-order correction.

Now, we derive the squeezing in the presence of loss, and investigate whether the relation between the initial growth rate and Petermann factor remains valid. We define the single-mode quadrature operator $X_\mu(\phi) = (a_\mu e^{-i\phi} + a_\mu^\dagger e^{i\phi})/\sqrt{2}$ for $\mu = 1, 2$. Since the state remains Gaussian, it is natural to quantify the degree of squeezing by defining an effective squeezing parameter $r(t)$ via $r(t) \equiv -\frac{1}{2} \ln V_-(t)$, where $V_-(t)$ denotes the minimum variance of the Einstein-Podolsky-Rosen (EPR) operator $X_-(\phi) \equiv X_1(\phi) - X_2(\phi)$. Note that this definition reduces to the squeezing parameter r defined in the ideal unstable case in the previous section, when the loss goes to 0. Direct calculation yields

$$V_-(t) = (2n + 1) - 2|m|,\tag{S65}$$

where we have used the relations $\langle a_1^2 \rangle = \langle a_2^2 \rangle = 0$, and $\langle a_1 a_2^\dagger \rangle = \langle a_1^\dagger a_2 \rangle = 0$.

Now, we can use the explicit value of $n(t)$ and $|m(t)|$ and examine the leading-order behavior of the squeezing parameter. Expanding to the first order (where $n(t) \sim \mathcal{O}(t^2)$ is negligible and $|m(t)| \approx |\Delta|t$, we obtain $V_-(t) \approx 1 - 2|\Delta|t$. Relating it to the squeezing parameter in the regime $g < |\Delta|$ and using the relation $K = |\Delta|^2/\kappa^2$ gives

$$r(t) = \sqrt{K}\kappa t + \mathcal{O}(t^2), \quad (\text{S66})$$

showing that for a fixed intrinsic growth rate κ , the enhancement factor \sqrt{K} of the initial squeezing rate persists even in the presence of uniform loss. Therefore, the transient behavior at early time $t \ll \gamma^{-1}$ gives the desired relation between the initial squeezing rate and the Petermann factor.

Crucially, the relation remains valid even in regime (ii). Although this regime corresponds to an intrinsically unstable system that is stabilized by loss, the initial squeezing behavior is still determined by the Petermann factor, which is associated with the exceptional point $g = |\Delta|$.

* These authors contributed equally to this work.

† kunx@cau.ac.kr

‡ bmin@kaist.ac.kr

- [1] A. Wünsche, [Journal of Optics B: Quantum and Semiclassical Optics](#) **2**, 73 (2000).
- [2] J. E. Sustaeta-Osuna, F. J. García-Vidal, and P. A. Huidobro, [ACS Photonics](#) **12**, 1873 (2025).
- [3] S. Inglima and B. J. Schroers, [Lett. Math. Phys.](#) **109**, 1433 (2019), arXiv:1804.05782 [hep-th].